The good? The bad? The mutant! Characterization of cancer-related somatic mutations and identification of a selectivity hotspot in adenosine receptor

Wang, X.

Chapter 4

Characterization of cancer-related somatic mutations in the adenosine A_{2B} receptor.

This chapter is based upon:
Xuesong Wang*, Willem Jespers*, Brandon J. Bongers, Maria C. C. Habben Jansen, Chantal M. Stangenderger, Majlen A. Dilweg, Hugo Gutiérrez-de-Terán, Adriaan P. IJzerman, Gerard J.P. van Westen and Laura H. Heitman
European Journal of Pharmacology. **2020**, 880:173126
** These authors contributed equally*

Abstract

In cancer, G protein-coupled receptors (GPCRs) are involved in tumor progression and metastasis. In this study we particularly examined one GPCR, the adenosine A_{2B} receptor. This receptor is activated by high concentrations of its endogenous ligand adenosine, which suppresses the immune response to fight tumor progression. A series of adenosine A_{2B} receptor mutations were retrieved from the Cancer Genome Atlas harboring data from patient samples with different cancer types. The main goal of this work was to investigate the pharmacology of these mutant receptors using a 'single-GPCR-one-G protein' yeast assay technology. Concentration-growth curves were obtained with the full agonist NECA for the wild-type receptor and 15 mutants. Compared to wild-type receptor, the constitutive activity levels in mutant receptors F141L$^{4.61}$, Y202C$^{5.58}$ and L310P$^{8.63}$ were high, while the potency and efficacy of NECA and BAY 60-6583 on Y202C$^{5.58}$ was lower. A 33- and 26-fold higher constitutive activity on F141L$^{4.61}$ and L310P$^{8.63}$ was reduced to wild-type levels in response to the inverse agonist ZM241385. These constitutively active mutants may thus be tumor promoting. Mutant receptors F259S$^{6.60}$ and Y113F$^{34.53}$ showed a more than one log-unit decrease in potency. A complete loss of activation was observed in mutant receptors C29R$^{1.54}$, W130C$^{4.50}$ and P249L$^{6.50}$. All mutations were characterized at the structural level, generating hypotheses of their roles on modulating the receptor conformational equilibrium. Taken together, this study is the first to investigate the nature of adenosine A_{2B} receptor cancer mutations and may thus provide insights in mutant receptor function in cancer.

Keywords: G protein-coupled receptor, Cancer-related mutations, yeast system

Introduction

G protein-coupled receptors (GPCRs) are a family of membrane-bound proteins that have seven-transmembrane (7TM) domains, connected by three intracellular (IL) and three extracellular (EL) loops, an extracellular amino terminus, and an intracellular carboxyl terminus[1]. GPCRs are responsive to a diverse set of physiological endogenous ligands including hormones and neurotransmitters. In total approximately 800 GPCRs are present in the human genome which can be subdivided in five main families, namely glutamate, rhodopsin, adhesion, frizzled/taste, and secretin, according to the GRAFS classification system[2].

GPCRs have been relatively underappreciated in preclinical oncology, where primary focus over the last two decades has been on kinases due to their central role in the cell cycle. However, there is a growing body of evidence showing a more prominent role of GPCRs in all phases of cancer[3]. In addition, recent work has shown that the function of GPCRs present in patient isolates is altered due to mutation, and indeed GPCRs are mutated in an estimated 20% of all cancers[4,5].

One particular class of rhodopsin-like GPCRs are the adenosine receptors (ARs), which respond to adenosine as their natural ligand[6]. There are four adenosine receptor subtypes, namely A_1, A_{2A}, A_{2B}, and A_3. The adenosine A_1 and A_3 receptors couple to the G_i protein and consequently inhibit adenylate cyclase and cAMP production. Conversely adenosine A_{2A} and A_{2B} receptors activate adenylate cyclase via coupling to the G_s protein[6,7]. While the role of the immune system in cancer defense is vital, the underlying mechanisms are yet not very well understood[8]. However, studies in immune cells provide evidence for the involvement of adenosine and adenosine receptors in these mechanisms[9]. Additionally, increased concentrations of adenosine are present in the tumor microenvironment. Hence adenosine may activate all subtypes of the adenosine receptors in cancer, including the low-affinity adenosine A_{2B} receptor[10].

Adenosine A_{2B} receptors expressed in human microvascular cells are likely modulating expression of angiogenic factors like vascular endothelial growth factor, interleukin-8 and basic fibroblast growth factor[11,12]. In HT29 colon[13], U87MG glioblastoma[14] and A375 melanoma cancer cells[15], increased interleukin-8 levels were observed after stimulation of adenosine A_{2B} receptor resulting in cell proliferation. Moreover, it has been suggested that adenosine A_{2B} receptors also regulate immunosuppression in the tumor microenvironment[16,17]. Recently, constitutive activity of the adenosine A_{2B} receptor has been determined and proven to be involved in the promotion of cell proliferation in prostate cancer[18]. Furthermore, the adenosine A_{2B} receptor is frequently overexpressed in oral squamous cell carcinoma and triple negative breast cancer cell lines, and promotes cancer progression[19,20]. On the other hand, it was shown that this receptor inhibits ERK 1/2 phosphorylation, resulting in an anti-proliferative action in ER-negative MDA-MB-231 cells[21]. However, a more recent study provided evidence for enhanced MAPK signaling via activation of the A_{2B}

receptor, promoting tumor progression in bladder urothelial carcinoma[22]. Taken all evidences together, it appears that activation of the adenosine A_{2B} receptor promotes tumor progression[23,24].

From a mechanistic point of view, it has been shown that mutations in this receptor can result in altered constitutive and agonist-induced receptor activity[25–28]. Mutant receptors that show increased basal activity independent of an agonist, are referred to as constitutively active mutants (CAMs), while those with decreased basal activity are termed constitutively inactive mutants (CIMs)[26]. Based on the two-state-receptor model[29], the equilibrium between the inactive (R) and active (R*) receptor conformation is shifted in these CAMs and CIMs.

In the present study, we selected 15 mutations in adenosine A_{2B} receptor from all cancer types using a bioinformatics approach. Subsequently these mutations were screened in an *S.cerevisiae* strain to study the effect of these mutations on receptor activation using different reference ligands (Fig. 1). We found that these mutations resulted in 3 CAMs and 5 less active mutants. Moreover, we found 4 mutants that behaved similar to the wild-type receptor (i.e. no effect mutants) and 3 loss-of-function mutants. Taken together, this study is the first to characterize cancer mutations on adenosine A_{2B} receptor at the molecular level and may thus provide insights in mutant receptor function in cancer.

Methods

Data mining

Mutation data from The Cancer Genome Atlas (TCGA, version August 8th 2015) was downloaded using Firehose[30,31]. Subsequently the data was extracted, when available MutSig 2.0 data was used, in cases where this was not available MutSig 2CV was used (specifically Colon Adenocarcinoma, Acute Myeloid Leukemia, Ovarian Cerous Cystadenocarcinoma, Rectum Adenocarcinoma). Natural variance mutation data was downloaded from Uniprot in the form of 'Index of Protein Altering Variants' (version November 11th 2015)[32].Sequence data was filtered for missense somatic mutations and the protein of interest (human A_{2B} receptor, Uniprot accession P29275)[33]. The GPCRdb alignment tool was used to assign Ballesteros Weinstein numbers[34,35], indicated by superscripts after the corresponding residue number. Finally, 15 cancer-related mutations were identified of which one mutation (L310P) was a duplicate, i.e. present in samples from two separate patients both suffering from colon adenocarcinoma.

Materials

The MMY24 strain, the S. *cerevisiae* expression vectors, the pDT-PGK plasmid, and the wild-type human adenosine A_{2B} receptor in pDT-PGK plasmid were kindly provided by Dr. Simon Dowell from GSK (Stevenage, UK). The QuikChange II® Site-

Directed Mutagenesis Kit was purchased from Agilent Technologies, which includes XL10-Gold ultracompetent cells (Amstelveen, the Netherlands). The QIAprep mini plasmid purification kit was purchased from QIAGEN (Amsterdam, the Netherlands). NECA (Fig. 1), 3-amino-[1,2,4]-triazole (3-AT), bovine serum albumin (BSA) and 3, 3',5,5'-tetramethyl-benzidine (TMB) were purchased from Sigma-Aldrich (Zwijndrecht, the Netherlands). BAY 60-6583 (Fig. 1) was synthesized in house. ZM241385 was purchased from Ascent Scientific (Bristol, United Kingdom). PSB603 (Fig. 1) was purchased from TOCRIS Bioscience (Abingdon, United Kingdom). The Hybond-ECL membrane and the ECL Western blotting analysis system were purchased from GE Healthcare (Eindhoven, the Netherlands). The antibody directed against the C-terminal region of the human adenosine A_{2B} receptor was kindly provided by Dr. I. Feoktistov (Vanderbilt University, Nashville, TN, USA), the antibody directed against the extracellular region of the human adenosine A_{2B} receptor was purchased from Alpha Diagnostic International (San Antonio, USA) and goat anti-rabbit IgG was purchased from Jackson ImmunoResearch Laboratories (West Grove, PA, USA).

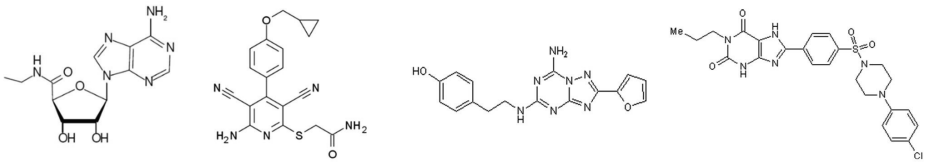

A. NECA B. BAY 60-6583 C. ZM241385 D. PSB 603

Fig 1. Structures of four reference compounds for the adenosine A_{2B} receptor: (A) agonist NECA, (B) non-ribose agonist BAY 60-6583, (C) inverse agonist ZM241385 and (D) neutral antagonist PSB603.

Generation of human adenosine A_{2B} receptor mutations

The mutations were generated as described previously by Liu *et al*[25]. In short, DNA primers for the human adenosine A_{2B} receptor (uniprot: P29275) mutations were designed by the QuikChange Primer Design Program of Agilent Technologies (Santa Clara, CA, USA). These primers contained a single substitution resulting in a codon change for the desired amino acid substitution. Primers and their complements were synthesized (Eurogentec, Maastricht, the Netherlands) and used to generate mutation plasmids according to the QuikChange method from Agilent Technologies. The mutagenic PCR was performed in the presence of 50 ng of template DNA, 10 µM concentration of each primer, 1 µl of dNTP mix, 2.5 µl of 10 x reaction buffer and 2.5 U *PfuUtra* HF DNA polymerase. The number of mutagenic PCR cycles was set to 22 (PCR cycling conditions: 95 °C for 30 s, 55 °C for 1 min, and 68 °C for 10 min). The methylated or hemimethylated non-mutated plasmid DNA was removed by 5 U *Dpn* I restriction enzyme incubating for 2 h at 37 °C. The mutated DNA plasmids were transformed into XL-1 Blue supercompetent cells according to the manual of the QuikChange II® Site-Directed Mutagenesis Kit. After plasmid isolation by using a QIAprep mini plasmid purification kit, the mutations were verified by double-strain

DNA sequencing (LGTC, Leiden University, the Netherlands).

Transformation in a MMY24 S. cerevisiae strain

The yeast strain was derived from the MMY11 strain and further adapted to communicate with mammalian GPCRs through a specific Gpa1p/$G_{\alpha i3}$ chimeric G protein. The genotype of the MMY24 is: **MATa** *his3 leu2 trp1 ura3 can1 gpa1_::G_i3 far1 ::ura3 sst2_::ura3 Fus1::FUS1-HIS3 LEU2::FUS1-lacZ ste2_::G418R* and the last five amino acid residues of C-terminus of Gpa1p/ $G_{\alpha i3}$ chimera were replaced by the same length sequence from mammalian $G_{\alpha i3}$ protein[36]. The pheromone pathway was coupled to HIS3 reporter gene via FUS1 promotor, so that the level of receptor activation can be measured directly by the yeast growth rate on histidine-deficient medium. The plasmids containing the mutant adenosine A_{2B} receptors were transformed into an S. *cerevisae* strain according to the Lithium-Acetate procedure [37].

Solid growth assay

To characterize the activation of various mutated receptors, concentration-growth curves were generated from a solid growth assay. This assay was performed with yeast cells from an overnight culture in selective YNB medium lacking uracil and leucine (YNB-UL) as this yeast strain can produce leucine and the plasmid also contains a gene encoding for uracil production. The yeast cells were diluted to 400,000 cells/ml (OD_{600} ≈ 0.02) and droplets of 1.5 µl were spotted on selection agar plates, i.e. YNB agar medium lacking uracil, leucine and histidine (YNB-ULH). In addition, the agar on the plates contained 7mM 3-AT and the adenosine A_{2B} receptor full agonist NECA in a concentration range from 10^{-9} to 10^{-4} M, or the non-ribose adenosine A_{2B} receptor agonist BAY 60-6583[38] in a concentration range from 10^{-9} to 10^{-5} M, or the adenosine A_{2B} receptor inverse agonist ZM241385[39] in a concentration range from 10^{-9} to 10^{-5} M. After 50 h incubation at 30 °C, the plates were scanned and receptor activation-mediated yeast cell growth was quantified with ImageLab 5.2.1 software of a ChemiDoc MP Imaging System from Bio-Rad (Hercules, CA, USA). The level of yeast cell growth was calculated as the intensity of each spot after correction for local background on the plate.

Liquid growth assay and Schild-plot analysis

To characterize the mutant adenosine A_{2B} receptors further, similar concentration-growth curves were obtained using liquid YNB-ULH medium and 96-well plates. Yeast cells were inoculated in YNB-UL and diluted to $4 \cdot 10^6$ cells/ml (OD_{600} ≈ 0.2). To each well, 150 µl YNB-ULH medium containing 7 mM 3-AT, 2 µl various concentrations of ligands and 50 µl yeast cells were added. The 96-well plate was then incubated at 30 °C for 35 h in a Genios plate reader, and was shaken every 10 min at 300 rpm for 1 min to keep the cells in suspension. The level of yeast cell growth was determined by the optical density at a wavelength of 595 nm. For the wild-type adenosine A_{2B} receptor, mutant receptor F141L$^{4.61}$, Y202C$^{5.58}$ and L310P$^{8.63}$, concentration-growth curves of

NECA were generated in the absence or presence of different concentrations of the selective adenosine A_{2B} receptor antagonist PSB603.

Whole cell extracts and immunoblotting

In order to determine the expression level of the different mutant adenosine A_{2B} receptors in the MMY24 yeast strain, an immunoblotting method was used as described previously[25]. In short, whole cell protein extracts were prepared using trichloroacetic acid (TCA) from an overnight culture ($1.2 \cdot 10^8$ yeast cells). After two washing steps with 20% TCA, yeast cells were broken by thoroughly vortexing in the presence of glass beads. Then, a semi-automated electrophoresis technique (PhastSystem™, Amersham Pharmacia Biotech) was used to separate 4 µl (≈24 µg) of the yeast cell extract on a 12.5% SDS/PAGE gel. Subsequently the proteins were blotted on a Hybond-ECL membrane, where a rabbit anti-human adenosine A_{2B} receptor primary antibody was used directed against the C-terminus of the human adenosine A_{2B} receptor. The remaining unbound antibody was washed off the membranes repeatedly with TBST (0.05% Tween 20 in Tris-buffered saline), and the HRP-conjugated goat anti-rabbit IgG (Jackson ImmunoResearch Laboratories) was added. Via the ECL Western blotting analysis (GE Healthcare, the Netherlands), the specific human adenosine A_{2B} receptor bands were found at 29 kDa and 48 kDa, whereas a nonspecific band was detected at approximately 45 kDa, which was used as loading control. Densitometric analysis was performed by the volume analysis tool in the ImageLab 5.2.1 software from Bio-Rad (Hercules, CA, USA). The ratio between the intensity of specific human adenosine A_{2B} receptor protein bands and nonspecific protein band was determined, where the yeast strain carrying wild-type $hA_{2B}R$ was set to 100% and the yeast strain carrying the empty vector pDT-PGK was set to 0%.

Yeast enzyme-linked immunosorbent assay (ELISA)

Yeast ELISA was adapted from a method reported previously[40]. About $2 \cdot 10^7$ yeast cells were collected from an overnight culture in YNB-UL medium. The cells were blocked with 2% BSA in Tris-buffered saline (TBS), followed by 1 hour incubation with polyclonal rabbit anti-human adenosine A_{2B} receptor antibody (1:2000) in TBST containing 0.1% BSA at room temperature. After washing three times with TBST, HRP-conjugated goat anti-rabbit IgG (1:5000) was added and incubated for 1 h at room temperature. After removing the secondary antibody and washing the cells with TBS, TMB was added and incubated for 15 minutes in the dark. The reaction was stopped with 1 M H_3PO_4, and absorbance was read at 450 nm using a Wallac EnVision 2104 Multilabel reader (PerkinElmer).

Homology modelling

Homology models were generated using the GPCR-ModSim web-based pipeline for modeling GPCRs[41,42], available through http://open.gpcr-modsim.org/. Shortly, this webserver performs a multiple sequence alignment against a curated set of

crystalized GPCRs, divided in three categories: inactive, active-like and fully-active. The best templates are suggested based on the overall homology with the target sequence and the user can select between single-template or multi-template homology modeling. In this study, the adenosine A_{2A} receptor was the only template used to model the adenosine A_{2B} receptor, using the structures deposited with PDB codes 3EML for the inactive model, 2YDV for the active-like and 5G53 for the fully-active structure. After manual adjustment of the alignment of the extracellular loop 2 (ECL2) region, which is recommended due to the high variability within this loop region, homology models were created and sorted by the DOPHR scoring function by the server, using Modeller as a background engine[43]. The best model was finally selected among the top scored models based on visual inspection.

Data analysis

All experimental data were analyzed using GraphPad Prism 7.0 software (GraphPad Software Inc., San Diego, CA, USA). Solid and liquid growth assays were analyzed by non-linear regression using "log (agonist or inhibitor) vs. response (three parameters)" to obtain potency (EC_{50}), inhibitory potency (IC_{50}) and efficacy (E_{max}) values. For Schild-plot analysis, log[DR-1] was calculated by equation log[DR-1] = log[(A'/A)-1], where A' is the EC_{50} value obtained from the concentration-growth curves in the presence of antagonist, A is the EC_{50} value obtained from the concentration-growth curves in the absence of antagonist. pA_2 values were generated by using linear regression. Statistical evaluation was performed by a two-tailed unpaired Student's *t-test* between pEC_{50} or E_{max} values of mutant receptors and values of wild-type receptor obtained from the same experiments. All values obtained are means of at least three individual experiments performed in duplicate.

Results

Data mining and expression of mutants

In total 15 point mutations in the adenosine A_{2B} receptor were identified in cancer patient isolates by data mining the TCGA database on August 8th 2015. Three mutations were located at an extracellular loop (EL), two at an intracellular loop (IL), six in the 7-transmembrane domain and four at the C-terminus of the adenosine A_{2B} receptor. Of note, three mutations were found for position $L310^{8.63,}$ i.e. L310F, L310I and L310P, of which the latter was present in two separate patient isolates. In the natural variance set 16 point mutations were identified, namely $A35V^{1.60}$, $T37S^{12.49}$, $C72Y^{23.51}$, $A82T^{3.29}$, $I126T^{4.46}$, $L129I^{4.49}$, $G135R^{4.55}$, $C171S^{45.50}$, $L172P^{45.51}$, $R223W^{6.24}$, $R228W^{6.29}$, $K267E^{EL3}$, $R293W^{7.56}$, $R295Q^{8.48}$, $D296G^{8.49}$ and $R298H^{8.51}$. However, none of these were found to match any of the residue positions of the cancer-related mutations. All 15 cancer-related mutants were constructed and transformed into the MMY24 yeast strain, and showed overall receptor expression, as determined by Western blot analysis of whole cell lysates (Fig. 2A and Table S1). Besides, all

mutant receptors also showed cell surface expression, as determined by ELISA performed on intact yeast cells (Fig. 2B and Table S1).

Characterization of mutant adenosine A_{2B} receptors on receptor activation

To characterize the effects of the cancer-related mutations on receptor activation,

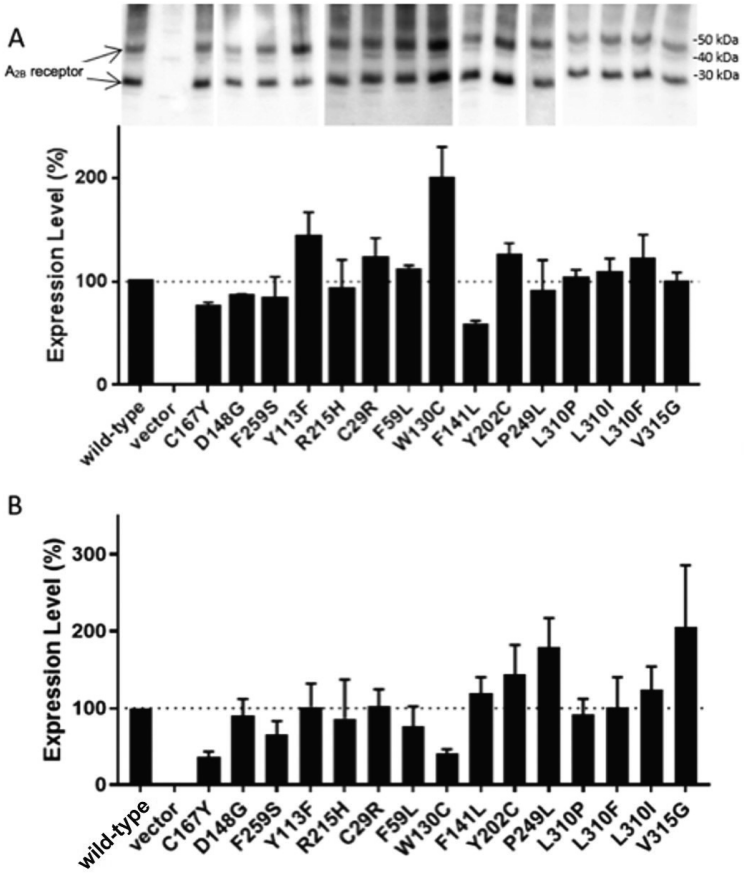

Fig 2. Expression levels of wild-type and mutant adenosine A_{2B} receptors. A) Western blot analysis of yeast transfected with vector in absence (vector) or presence of wild-type or 15 mutant adenosine A_{2B} receptors. The upper panel shows one representative blot, where the arrows indicate the specific human adenosine A_{2B} receptor bands at 29 kDa and 48 kDa. The lower panel shows the bar graph obtained from the densitometric analysis. Expression levels were determined between the density of specific bands and the density of the non-specific band that is present in all lanes. Wild-type receptor was set at 100% and the empty vector pDT-PGK was set at 0%. The combined bar graph is shown in mean ± SEM from at least three individual experiments. B) Representative experiment of cell surface expression levels of wild-type and mutant adenosine A_{2B} receptors, determined in an enzyme-linked immunosorbent assay. Wild-type receptor was set at 100% and the empty vector pDT-PGK was set at 0%. The bar graph is shown in mean ± SD of two individual experiment performed in duplicate. Table S1 has the full data set for two independent experiments.

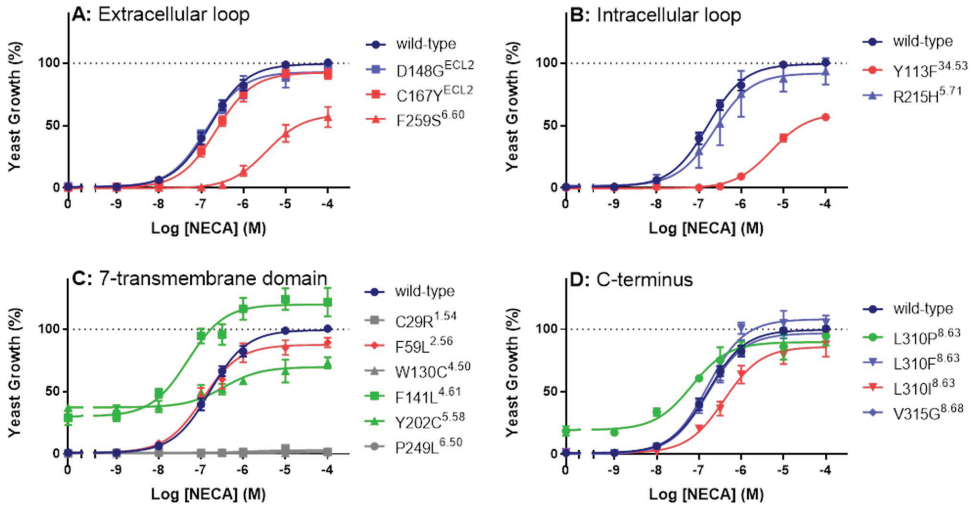

Fig 3. Concentration-response curves for NECA at the wildtype and 15 mutant adenosine A_{2B} receptors. Data is separated for mutations located on (A) extracellular loop, (B) intracellular loop, (C) 7-transmembrane domain and (D) C-terminus. The maximum activation level of wild-type adenosine A_{2B} receptor was set at 100%, while the background of the selection plate was set at 0%. Combined graphs are shown as mean ± SEM from at least three individual experiments, each performed in triplicate.

the pharmacology of these 15 mutant receptors was investigated by yeast-growth assays. Concentration-growth curves and results of the mutant receptors in response to the full agonist NECA are shown in Fig. 3 and Table 1.

In this system, the wild-type receptor showed a pEC_{50} value of 6.79±0.09 for NECA and a low level of basal activity, if any. Overall half of the mutant receptors showed similar constitutive activity, potency and efficacy as the wild-type receptors (Table 1). In the ECL and ICL, two mutants behaved significantly different from wild-type adenosine A_{2B} receptor in response to NECA, i.e. mutant receptor F259S$^{6.60}$ (Fig. 3A) and mutant receptor Y113F$^{34.53}$ (Fig. 3B) displayed a more than 1 log-unit decreased potency. The maximum receptor activation (E_{max}) of these two mutant receptors was also decreased to 57% for both (Table 1). At the 7-transmembrane domain of the adenosine A_{2B} receptor, mutants C29R$^{1.54}$, W130C$^{4.50}$ and P249L$^{6.50}$ showed a complete loss of function (Fig. 3C). In contrast, increased constitutive activities were observed for mutant receptors F141L$^{4.61}$ and Y202C$^{5.58}$, which were 34- and 48- fold higher than the wild-type receptor, respectively (Fig. 3C and Table 1). In response to NECA, mutant receptor F141L$^{4.61}$ showed a significantly increased potency with a pEC_{50} value of 7.31±0.03 and an increased E_{max} value of 122%, while mutant receptor Y202C$^{5.58}$ showed a significantly reduced pEC_{50} value of 6.30±0.09 and reduced E_{max} value of 73% in comparison to the wild-type receptor (Fig. 3C and Table 1). At the C-terminus, mutant receptor L310P$^{8.63}$ showed a relatively high level of constitutive activity, i.e. 26-fold higher than wild-type receptor, as well as an increased potency for NECA. Mutant receptor L310I$^{8.63}$ showed a significantly decreased pEC_{50} value

of 6.40±0.01 compared to wild-type receptor (Fig. 3D and Table 1), while the E_{max} value did not decrease significantly. Mutant receptor V315G$^{8.68}$ showed similar pEC_{50} and E_{max} values to wild-type receptor (Fig. 3D and Table 1), although the cell surface expression level was much higher than wild-type receptor (Fig. 2B). Additional yeast ELISA experiments were performed on yeast colonies carrying either wild-type or mutant receptor V315G$^{8.68}$, and colonies with similar expression levels were selected in yeast liquid growth assay to further investigate receptor activation in response to NECA. Interestingly, similar pEC_{50} and E_{max} values were still obtained for mutant receptor V315G$^{8.68}$ and wild-type adenosine A_{2B} receptor (Table S2).

The mutant receptors F259S$^{6.60}$, Y113F$^{34.53}$, C29R$^{1.54}$, W130C$^{4.50}$, P249L$^{6.50}$, F141L$^{4.61}$, Y202C$^{5.58}$ and L310P$^{8.63}$ which all showed the more altered pharmacological response to NECA were also studied with BAY 60-6583, a non-ribose adenosine A_{2B} receptor agonist (Fig. 1). On the wild-type receptor, BAY 60-6583 showed a pEC_{50} value of 7.49±0.33. As for NECA, decreased potencies and E_{max} values were also observed for BAY 60-6583 at F259S$^{6.60}$ and Y113F$^{34.53}$ in comparison to the wild-type receptor (Table 1). Mutant receptors C29R$^{1.54}$, W130C$^{4.50}$ and P249L$^{6.50}$, which did not show any activity in the presence of NECA, were not activated by BAY 60-6583 either (Table 1). As opposed to NECA, the effects of BAY 60-6583 on mutant receptors F141L$^{4.61}$, Y202C$^{5.58}$ and L310P$^{8.63}$ were similar when compared to the wild-type receptor (Table 1).

Taken together, based on the different pharmacological effects we characterized mutant receptors F141L$^{4.61}$, Y202C$^{5.58}$ and L310P$^{8.63}$ as CAMs, mutant receptors C29R$^{1.54}$, W130C$^{4.50}$ and P249L$^{6.50}$ as loss of function mutants (LFMs), mutant receptors C167Y^{ECL2}, F259S$^{6.60}$, Y113F$^{34.53}$, F59L$^{2.56}$ and L310I$^{8.63}$ as less active mutants (LAMs) and mutant receptors D148S^{ECL2}, R215H$^{5.71}$, L310F$^{8.63}$ and V315G$^{8.68}$ as no effect mutants (NEMs).

Inverse agonism of the CAMs

To study whether receptors bearing CAMs (F141L$^{4.61}$, Y202C$^{5.58}$ and L310P$^{8.63}$) could still be inhibited, an inverse agonist of the A_{2B} receptor, ZM241385, was used in the yeast solid growth assay, and compared to the wild-type receptor. The concentration-growth inhibition curves are shown in Fig. 4. The wild-type adenosine A_{2B} receptor had low basal activity in this system, and ZM241385 did not further reduce this. All CAMs displayed a decreased activity upon increasing concentrations of ZM241385. The level of constitutive activity of F141L$^{4.61}$ and L310P$^{8.63}$ was fully suppressed, with pIC_{50} values of 7.43±0.17 and 7.49±0.27 for ZM241385, respectively (Fig. 4 and Table 1). For the mutant receptor with the highest constitutive activity Y202C$^{5.58}$, ZM241385 caused a partial reduction to a residual activity of 19% and with a lower pIC_{50} of 6.62±0.23 than for the less active CAMs, i.e. F141L$^{4.61}$ and L310P$^{8.63}$ (Fig. 4).

Table 1. Characterization of adenosine A_{2B} receptor mutations identified in cancer patient samples in yeast solid growth assays. Mutations are shown in the numbering of the adenosine A_{2B} receptor amino acid sequence as well as according to the Ballesteros and Weinstein GPCR numbering system.

		NECA		BAY 60-6583		
Mutation	**Fold CA**	**pEC_{50}**	**E_{max} (%)**	**pEC_{50}**	**E_{max} (%)**	**Type**
wild-type	1.0	6.79±0.23	100±4	7.49±0.57	100±3	-
C167Y^{ECL2}	1.0	6.65±0.19	91±7*	-	-	LAM
D148G^{ECL2}	2.5	6.87±0.11	98±5	-	-	NEM
F259S$^{6.60}$	0.6	5.44±0.23****	57±14***	6.71±0.41	20±9$^{###}$	LAM
Y113F$^{34.53}$	0.6	5.28±0.12****	57±4****	6.51±0.45$^{#}$	15±1$^{####}$	LAM
R215H$^{5.71}$	2.8	6.57±0.48	94±18	-	-	NEM
C29R$^{1.54}$	1.1	ND	ND	ND	ND	LFM
F59L$^{2.56}$	1.0	6.94±0.23	89±7*	-	-	LAM
W130C$^{4.50}$	0.4	ND	ND	ND	ND	LFM
F141L$^{4.61}$	33	7.31±0.06**	122±19*	7.64±0.27	108±9	CAM
Y202C$^{5.58}$	48	6.30±0.15*	73±8***	7.21±0.18	74±18$^{#}$	CAM
P249L$^{6.50}$	0.4	ND	ND	ND	ND	LFM
L310P$^{8.63}$	26	7.21±0.14*	95±13	7.16±0.23	80±8$^{#}$	CAM
L310F$^{8.63}$	2.0	6.80±0.12	105±10	-	-	NEM
L310I$^{8.63}$	3.6	6.40±0.02*	88±17	-	-	LAM
V315G$^{8.68}$	1.4	6.89±0.19	94±4	-	-	NEM

pEC_{50} and E_{max} values are shown as mean ± SD from at least three individual experiments, each performed in triplicate. The percentage maximum effect (% E_{max}) and the fold constitutive activity values were calculated by the mean values generated from the concentration-growth curves, compared to the wild-type receptor. Dose-growth curves of BAY 60-6583 were only generated for mutants that responded significantly different to NECA in comparison to the wild-type receptor.

* $P < 0.05$, ** $P < 0.01$, *** $P < 0.001$, **** $P < 0.0001$ compared to the wild-type receptor in response to NECA; # $P < 0.05$, ### $P < 0.001$, #### $P < 0.0001$ compared to the wild-type receptor in response to BAY 60-6583, determined by a two-tailed unpaired Student's t-test.

ND: not detectable, -: not measured, CA: constitutive activity; CAM: constitutively active mutant, LAM: less active mutant, LFM: loss of function mutant, NEM: no effect mutant

Characterization of CAMs on ligand binding

To investigate whether the affinity of an antagonist had changed on the CAM receptors F141L$^{4.61}$, Y202C$^{5.58}$ and L310P$^{8.63}$, a Schild-plot analysis was performed (Fig. 5). Concentration-growth curves were generated of the agonist NECA in the absence or presence of increasing concentrations of the competitive adenosine A_{2B} receptor antagonist PSB603 (Fig. 1). For the wild-type and mutant receptors F141L$^{4.61}$ and L310P$^{8.63}$, a rightward shift of the concentration-growth curves was observed with increasing concentrations of PSB603 (Fig. 5A-C). This resulted in decreased apparent pEC_{50} values for NECA, while the maximal growth levels for

these mutant receptors were still reached. The pA_2 values, as determined from the Schild-plot, were 8.47 for wild-type, 8.07 for F141L$^{4.61}$ and 8.27 for L310P$^{8.63}$, showing that the antagonist affinity for these two mutants was not significantly influenced by the mutations (p = 0.0776 and p = 0.3097, respectively). Of note, a Schild-plot could not be generated for mutant receptor Y202C$^{5.58}$, as the presence of PSB603 (at the selected concentrations) did not cause a shift in agonist potency (Fig. 5D).

Structural mapping and analysis of mutations

The mutations investigated in this study were mapped on a homology model of the adenosine A_{2B} receptor to provide structural hypotheses for the observed pharmacological effect (NEM, LFM, CAM and LAM) of the different mutations. As illustrated in Figure 6A, the studied mutations are distributed over the whole receptor. The NEMs are positioned in the ECL, ICLs and C-terminus regions, while all three LFMs are exclusively located in the transmembrane region. These mutations are either part of highly conserved areas of the receptor (W130C$^{4.50}$ and P249L$^{6.50}$, Fig. 6C) and/or introduce a drastic change in the properties of the amino acid (C29R$^{1.54}$, W130C$^{4.50}$). The two LAMs are located in either the ECL (F259S$^{6.60}$, Fig. 6C) or ICL (Y113F$^{34.53}$, Fig. 6D) region, where F259$^{6.60}$ is located on the top of the helix 6, while Y113$^{34.53}$ is part of the TDY triad (see Discussion). Finally, the three CAMs are located in the transmembrane region or in helix 8. Mutant receptor L310P$^{8.63}$ has been identified in two individual patients. Additionally, mutations of this residue to Phe (F) and Ile (I) were found, where mutation to F did not alter receptor functionality. The F141L$^{4.61}$ mutation is positioned at the membrane-helix interface on the top of TM4 and at the start of ECL2. Noteworthy are the opposing pharmacological effects observed between F259S$^{6.60}$ and F141L$^{4.61}$ (i.e. LAM and CAM, respectively), although they are both situated at a structurally similar location. Y202$^{5.58}$ is part of an activation switch with Y290$^{7.53}$ in the NPxxY motif, moving outward into the membrane in the agonist-bound receptor as observed in the adenosine A_{2A} receptor crystal structures (Fig. 6B).

Discussion

Numerous GPCR mutations are known to alter the pharmacological function of the receptor by affecting constitutive activity, ligand binding, GPCR-G protein interaction, and / or cell surface expression, resulting in a wide range of disease phenotypes[44]. Moreover, a variety of mutations within GPCRs have been linked to different types of cancer[45–47], but the pharmacological effects of these cancer-related mutations are not yet fully understood. Previously, several studies performed on the adenosine A_{2B} receptor demonstrated some residues to be essential in receptor activation[25–28,35,48]. Hence, in this study 15 single-site point mutations of adenosine A_{2B} receptor identified from The Cancer Genome Atlas (TCGA)[31] were examined in the *S.cerevisiae* system to improve our understanding of the mechanism of receptor

activation in relation to cancer progression. As none of these mutations were found in the natural variance mutation dataset[32], they could be cancer specific, yet follow up research is warranted.

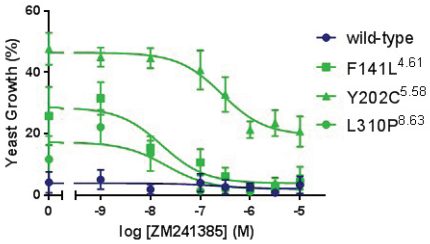

Fig 4. Concentration-inhibition curves of the adenosine A_{2B} receptor inverse agonist ZM241385 at the wild-type adenosine A_{2B} receptor and CAMs, F141L$^{4.61}$, Y202C$^{5.58}$ and L310P$^{8.63}$. The maximum activation level of wild-type adenosine A_{2B} receptor was set at 100%, the background of the selection plate was set at 0%. Combined graphs are shown from at least three individual experiments, each performed in triplicate.

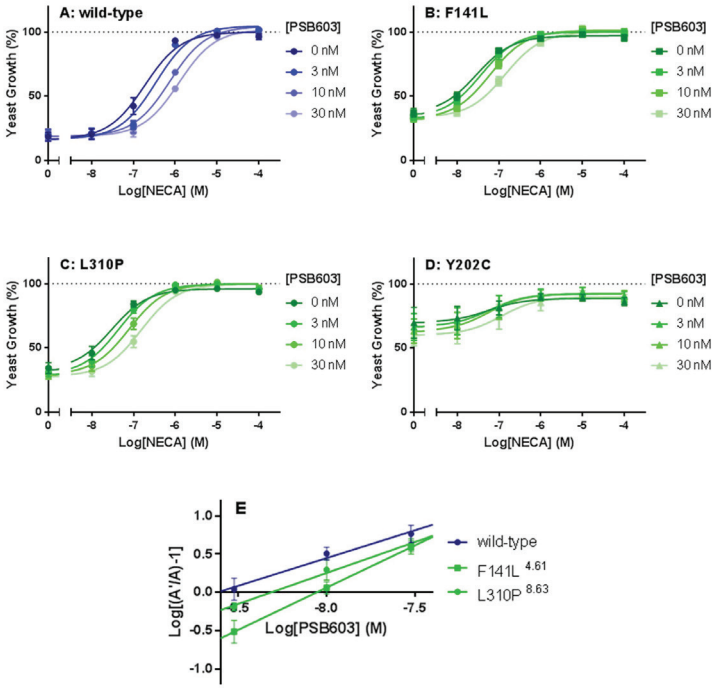

Fig 5. Schild analysis of adenosine A_{2B} receptor antagonist PSB603 binding to wild-type receptor and CAMs. Concentration-growth curves of NECA for (A) wild-type adenosine A_{2B} receptor, (B) F141L$^{4.61}$ Y202C$^{5.58}$, (C) L310P$^{8.63}$ and (D) Y202C$^{5.58}$ were obtained in the absence or presence of increasing concentrations of PSB603. (E) A Schild-plot to obtain pA_2 values of PSB603 on the wild-type and mutant receptors F141L$^{4.61}$ and L310P$^{8.63}$. Data are shown as mean ± SEM from at least three individual experiments, each performed in duplicate.

Less active mutants

Mutant receptors F259S$^{6.60}$ and Y113F$^{34.53}$ were identified from colon adenocarcinoma and lung adenocarcinoma located at opposite sides of the receptor, ECL3 and ICL2. However, both showed decreased potency and efficacy in the case of ribose and non-ribose agonists (Fig. 1 and Table 1, LAMs). These data are consistent with a previous study on the CC-chemokine receptor 5 (CCR5) receptor, showing that mutation from phenylalanine to alanine at position 6.60 resulted in a decreased affinity of the agonist gp120[49].

Residue Y113$^{34.53}$ is completely conserved among adenosine receptors and several other class A GPCRs. Structures of the adenosine A_1 and A_{2A} receptor show that this residue is part of a conserved triad (T$^{2.39}$–D$^{3.49}$–Y$^{34.53}$). We and others previously hypothesized a regulatory role of this motif in receptor activation [35] by mediating the strength of the D102-R103 ionic lock[50,51], preventing an outward movement of R$^{3.50}$ necessary for G protein binding (Fig. 6D). The Y113F$^{34.53}$ mutation increases the electrostatic attraction between D102$^{3.49}$ and R103$^{3.50}$, reducing the mobility of this residue. Notably, at the same position in the β_1-adrenergic receptor, mutation Y149A$^{34.53}$ leads to a large decrease in thermal stability of the antagonist bound state of the receptor[52].

Loss of function mutants

Mutant receptors C29R$^{1.54}$, W130C$^{4.50}$ and P249L$^{6.50}$, identified from stomach adenocarcinoma, liver hepatocellular carcinoma, and colon adenocarcinoma, respectively, showed a complete loss of activation (Fig. 3C and Table 1). Importantly, none of these mutant receptors showed severely reduced expression levels compared to the wild-type receptor (Fig. 2A and B, Table S1), indicating that the loss of activation is not due to the loss of expression in our model system. At residue C1.54, a drastic change from cysteine to arginine resulted in a LFM in our study. At the same position (1.54) in CCR2 and CCR5, the conservative mutation CCR2-V62I$^{1.54}$ did not affect receptor expression or ligand binding[53], yet the inverse mutation on CCR5-I52V$^{1.54}$ showed a decreased affinity for CCL5[54].

The tryptophan at position 130$^{4.50}$ and proline at position 249$^{6.50}$ are highly conserved among all class A GPCRs with a presence of 96% and 100%[55]. Mutant W4.50Cinvestigated on CXCR4 and melanocortin-4 receptor (MC4R) showed abolished ligand binding and cAMP response[56,57], indicating that the introduction of a drastic change in the amino acid properties at highly conserved positions can dramatically change receptor functionality. A rigid body motion of TM6 related to TM3 is known to be facilitated through the presence of the conserved proline in TM6 (6.50)[58]. Pro$^{6.50}$ is also known as a rotamer toggle switch, playing a role in the structural rearrangement of class A GPCRs on transition from the inactive to the active state (Fig. 6C)[59]. Hence the observed loss of function for the mutations at positions 130$^{4.50}$ and 249$^{6.50}$ has some precedent.

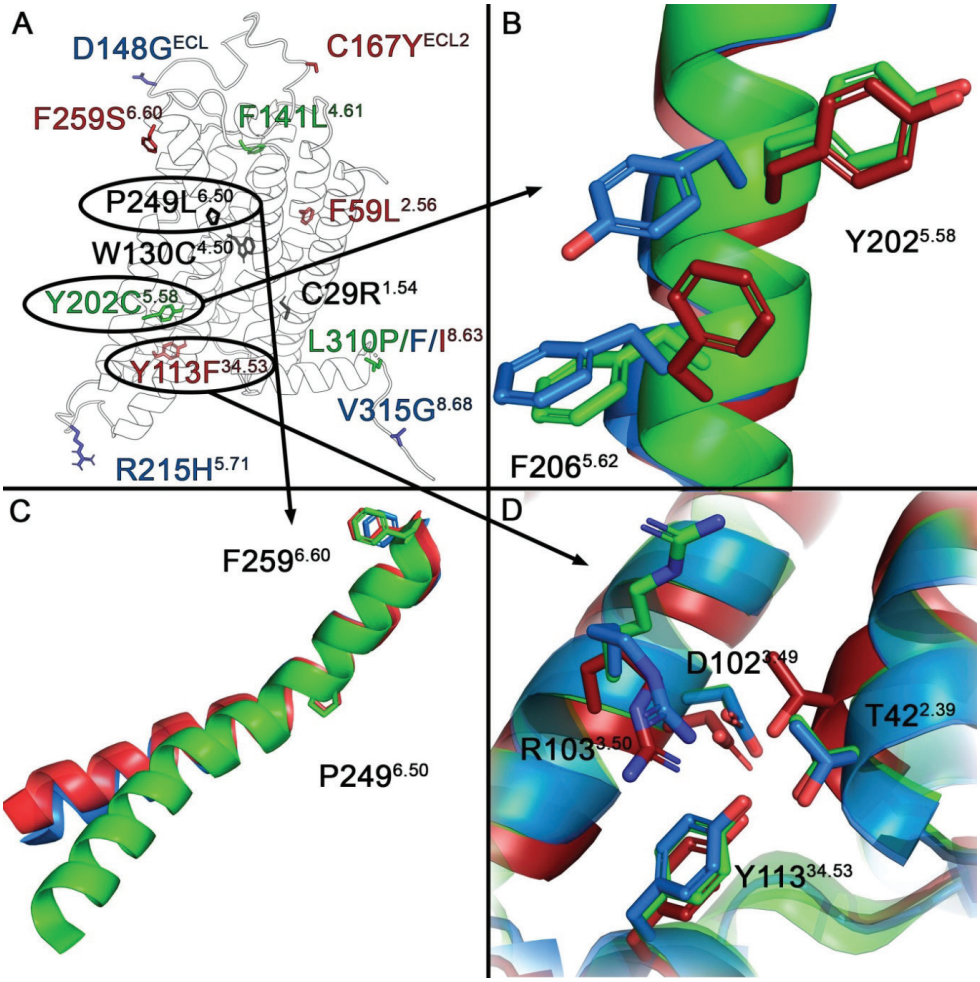

Fig 6. (A) Homology model of the adenosine A_{2B} receptor, showing the mutated residues subject of analysis. Color code is green for constitutively active mutants; black for loss-of-function mutants; red for less active mutants; and blue for no-effect-mutants. Panels (B, C and D) zoom in on selected residues mapped on the respective conformational models (inactive: orange, generated with 3eml; active-like: blue, generated with 2ydv; active: green, generated with 5g53). (B) The CAM Y202C$^{5.58}$ is located on part of an activation switch, which moves outwards to the membrane in the active-like structure and again inwards in the active structure, simultaneously F206$^{5.62}$ moves out in the active-like structure but remains in this position in the active structure. (C) The loss-of-function mutant P249L$^{6.50}$ disturbs a hinge region in the outward movement of TM6 observed upon receptor activation. (D) The less active mutant Y113F$^{34.53}$ is proposed to prevent the outward movement of R103$^{3.50}$ observed upon receptor activation.

Constitutively active mutants

Mutant receptors F141L$^{4.61}$, Y202C$^{5.58}$ and L310P$^{8.63}$, identified from skin cutaneous melanoma, liver hepatocellular carcinoma, and colon adenocarcinoma, respectively, showed increased constitutive activities compared to the wild-type receptor (Fig. 3 and Table 1). These CAMs are located at TM4, TM5, and helix 8. It is known that

TM4, TM5, ECL2, and helix 8 of the receptor are involved in receptor activation[25,60]. Upon activation, a coupling between movements of ECL2 and TM5 has been observed as well as a rearrangement in the H-bond networks connecting ECL2 with the extracellular ends of TM4, TM5 and TM6[61]. Among the CAMs in this study, constitutive activities of F141L$^{4.61}$ and L310P$^{8.63}$ were reduced to wild-type level by inverse agonist ZM241385 with pIC_{50} values of 7.43 and 7.49 (Fig. 4). These values are comparable to reference pK_i values for wild-type adenosine A_{2B} receptor in the cAMP assay[62,63]. However, ZM241385 reduced the high constitutive activity of Y202C$^{5.58}$ roughly by half (Fig. 4), demonstrating that adenosine A_{2B} receptor is locked in an active conformation by mutation Y202C$^{5.58}$, but not by F141L$^{4.61}$ or L310P$^{8.63}$. Concordantly, PSB603 did not significantly inhibit the Y202C$^{5.58}$ mutant in a Schild-plot analysis at concentrations that inhibited the other two mutants (Fig. 5). Such "locked-in" receptor mutants have been described before, e.g. for the adenosine A_1 receptor[64]. An altered potency value of NECA was observed on these CAMs compared to wild-type, while this difference was absent with BAY 60-6583 (Table 3). Similar results have been reported on adenosine A_{2A} receptor[65]. The difference in receptor activation among wild-type and mutant receptors in response to CGS21680 (a ribose agonist) was not seen upon the activation mediated by LUF5834 (a non-ribose agonist).

F141L$^{4.61}$, located at the membrane-helix interface on the top of TM4 and at the start of ECL2 (Figure 6A), has been reported to increase affinity and potency for NECA and BAY 60-6583 in a random mutagenesis study[28]. Similar results were observed here (Fig. 3C and Table 1), while no significant changes on affinity of PSB603 were observed (Fig. 5E). As residue F141$^{4.61}$ is not located at the binding pocket of either NECA or BAY 60-6583[66] but still able to affect agonist activation, it is therefore likely that this mutation plays a role in the stabilization of ECL2[28] and also participates in the entry conformation of the agonist binding pocket. Interestingly, opposite pharmacological effects were observed between F259S$^{6.60}$ and F141L$^{4.61}$, both situated at a structurally similar position (Figure 3A, 3C, 6A and Table 1).

Three mutations were identified at "hotspot" L310$^{8.63}$. L310P showed increased constitutive activity and potency on NECA, while L310F and L310I did not dramatically alter receptor functionality. Interestingly, the introduction of a proline mutation has a high impact as it may introduce a kink in helix 8, and thus potentially affect G protein coupling.

Residue Y5.58 is completely conserved among adenosine receptors and 88% conserved among class A GPCRs. Mutant receptor Y202C$^{5.58}$ showed the highest constitutive activity and reduced potency and efficacy of NECA compared to the wild-type receptor (Figure 3C and Table 1), indicating that maximal G protein coupling and signaling were decreased but consistently present. The residues Y$^{7.53}$ (part of NPxxY motif) and Y$^{5.58}$ were previously proposed as a possible activation switch for adenosine receptors, based on conformational changes observed in the agonist bound crystal structure[67] and their high conservation in class A GPCRs[51]. Comparing

the inactive and active structures of adenosine A_{2A} receptor (PDB: 3EML, 2YDV and 5G53), we noticed the side chain of $Y197^{5.58}$ stretched into the membrane in the active structures[67–69]. As a consequence, TM5 and TM6 moved closer together enabling access of the G protein (Figure 6B). Upon G protein binding, $Y197^{5.58}$ moves back into the receptor interior, filling up a space previously occupied by $L235^{6.37}$ and $I238^{6.40}$. Additionally, the constitutive activities of the mutated receptors Y202C and Y202S[28] are high, but not higher than the maximum observed effect of agonist bound receptors, further providing evidence that this residue is key for controlled modulation of the receptor.

Conclusion

In conclusion, 15 cancer-related somatic mutations on the adenosine A_{2B} receptor were retrieved from TCGA and characterized in a robust yeast system. We identified mutations that dramatically change receptor activation and function. Mutations in the adenosine A_{2B} receptor showing altered function in the yeast system may also be associated with cell proliferation and migration in cancer cell lines, and involved in cancer progression. Further studies in mammalian and/or cancer cell lines are warranted starting from the results in the present study to investigate mutation-mediated receptor activation and inactivation in a pathological setting. Since adenosine is an anti-inflammatory stimulus in the tumor microenvironment[10], both wild-type and mutant adenosine receptors may play an important, yet largely undefined role in cancer progression, which eventually may be modulated with medicinal products.

References

1. Vassilatis, D. K. *et al.* The G protein-coupled receptor repertoires of human and mouse. *Proc. Natl. Acad. Sci.* **100**, 4903–4908 (2003).
2. Fredriksson, R., Lagerström, M. C., Lundin, L.-G. & Schiöth, H. B. The G-protein-coupled receptors in the human genome form five main families. Phylogenetic analysis, paralogon groups, and fingerprints. *Mol. Pharmacol.* **63**, 1256–72 (2003).
3. Lappano, R. & Maggiolini, M. GPCRs and cancer. *Acta Pharmacol. Sin.* **33**, 351–362 (2012).
4. Watson, I. R., Takahashi, K., Futreal, P. A. & Chin, L. Emerging patterns of somatic mutations in cancer. *Nat. Rev. Genet.* **14**, 703–18 (2013).
5. Kan, Z. *et al.* Diverse somatic mutation patterns and pathway alterations in human cancers. *Nature* **466**, 869–73 (2010).
6. Fredholm, B. B. Adenosine receptors as drug targets. *Exp. Cell Res.* **316**, 1284–1288 (2010).
7. Fredholm, B. B., Irenius, E., Kull, B. & Schulte, G. Comparison of the potency of adenosine as an agonist at human adenosine receptors expressed in Chinese hamster ovary cells. *Biochem. Pharmacol.* **61**, 443–8 (2001).
8. M. Candeias, S. & S. Gaipl, U. The Immune System in Cancer Prevention, Development and Therapy. *Anticancer. Agents Med. Chem.* **16**, 101–107 (2015).
9. Antonioli, L. *et al.* Adenosine and inflammation: what's new on the horizon? *Drug Discov. Today* **19**, 1051–1068 (2014).
10. Gessi, S., Merighi, S., Sacchetto, V., Simioni, C. & Borea, P. A. Adenosine receptors and cancer. *Biochim. Biophys. Acta* **1808**, 1400–1412 (2011).
11. Fredholm, B. B., IJzerman, A. P., Jacobson, K. a, Klotz, K. N. & Linden, J. International Union of Pharmacology. XXV. Nomenclature and classification of adenosine receptors. *Pharmacol. Rev.* **53**, 527–52 (2001).
12. Feoktistov, I. *et al.* Differential expression of adenosine receptors in human endothelial cells: role of A_{2B} receptors in angiogenic factor regulation. *Circ. Res.* **90**, 531–8 (2002).
13. Merighi, S. *et al.* Caffeine Inhibits Adenosine-Induced Accumulation of Hypoxia-Inducible Factor-1α, Vascular Endothelial Growth Factor, and Interleukin-8 Expression in Hypoxic Human Colon Cancer Cells. *Mol. Pharmacol.* **72**, 395–406 (2007).
14. Zeng, D. *et al.* Expression and function of A_{2B} adenosine receptors in the U87MG tumor cells. *Drug Dev. Res.* **58**,

405–411 (2003).
15. Merighi, S. *et al.* Pharmacological and biochemical characterization of adenosine receptors in the human malignant melanoma A375 cell line. *Br. J. Pharmacol.* **134**, 1215–1226 (2001).
16. Ryzhov, S. *et al.* Host A_{2B} receptors promote carcinoma growth. *Neoplasia* **10**, 987–995 (2008).
17. Sorrentino, C., Miele, L., Porta, A., Pinto, A. & Morello, S. Myeloid-derived suppressor cells contribute to A_{2B} adenosine receptor-induced VEGF production and angiogenesis in a mouse melanoma model. *Oncotarget* **6**, 27478–27489 (2015).
18. Vecchio, E. a. *et al.* Ligand-Independent Adenosine A_{2B} Receptor Constitutive Activity as a Promoter of Prostate Cancer Cell Proliferation. *J. Pharmacol. Exp. Ther.* **357**, 36–44 (2016).
19. Kasama, H. *et al.* Adenosine A_{2b} receptor promotes progression of human oral cancer. *BMC Cancer* **15**, 563-575 (2015).
20. Mittal, D. *et al.* Adenosine 2B Receptor Expression on Cancer Cells Promotes Metastasis. *Cancer Res.* **76**, 4372–4382 (2016).
21. Bieber, D., Lorenz, K., Yadav, R. & Klotz, K.-N. A_{2B} adenosine receptors mediate an inhibition of ERK1/2 phosphorylation in the breast cancer cell line MDA-MB-231. *Naunyn-Schmiedebergs Arch Pharmacol* **377**, 1–98 (2008).
22. Zhou, Y. *et al.* The adenosine A_{2B} receptor promotes tumor progression of bladder urothelial carcinoma by enhancing MAPK signaling pathway. *Oncotarget* **8**, 48755–48768 (2017).
23. Sepúlveda, C., Palomo, I. & Fuentes, E. Role of adenosine A_{2b} receptor overexpression in tumor progression. *Life Sci.* **166**, 92–99 (2016).
24. Allard, B., Beavis, P. A., Darcy, P. K. & Stagg, J. Immunosuppressive activities of adenosine in cancer. *Curr. Opin. Pharmacol.* **29**, 7–16 (2016).
25. Liu, R., Nahon, D., le Roy, B., Lenselink, E. B. & IJzerman, A. P. Scanning mutagenesis in a yeast system delineates the role of the NPxxY(x)5,6F motif and helix 8 of the adenosine A_{2B} receptor in G protein coupling. *Biochem. Pharmacol.* **95**, 290–300 (2015).
26. Peeters, M. C. *et al.* GPCR structure and activation: an essential role for the first extracellular loop in activating the adenosine A_{2B} receptor. *FASEB J.* **25**, 632–43 (2011).
27. Peeters, M. C. *et al.* Domains for activation and inactivation in G protein-coupled receptors--a mutational analysis of constitutive activity of the adenosine A_{2B} receptor. *Biochem. Pharmacol.* **92**, 348–57 (2014).
28. Peeters, M. C., Li, Q., van Westen, G. J. P. & IJzerman, A. P. Three 'hotspots' important for adenosine A_{2B} receptor activation: a mutational analysis of transmembrane domains 4 and 5 and the second extracellular loop. *Purinergic Signal.* **8**, 23–38 (2012).
29. Leff, P. The two-state model of receptor activation. *Trends Pharmacol. Sci.* **16**, 89–97 (1995).
30. Weinstein, J. N. *et al.* The Cancer Genome Atlas Pan-Cancer analysis project. *Nat. Genet.* **45**, 1113–1120 (2013).
31. *Broad Institute TCGA Genome Data Analysis Center (2016): Analysis-ready standardized TCGA data from Broad GDAC Firehose stddata_2015_08_21 run. Broad Institute of MIT and Harvard.* (2016). doi:10.7908/C18W3CNQ
32. The 1000 Genomes Project Consortium. A global reference for human genetic variation. *Nature* **526**, 68–74 (2015).
33. UniProt: the universal protein knowledgebase. *Nucleic Acids Res.* **45**, D158–D169 (2017).
34. Ballesteros, J. A. & Weinstein, H. Integrated methods for the construction of three-dimensional models and computational probing of structure-function relations in G protein-coupled receptors. in *Methods in Neurosciences* **25**, 366–428 (1995).
35. Isberg, V. *et al.* GPCRdb: an information system for G protein-coupled receptors. *Nucleic Acids Res.* **44**, D356–D364 (2016).
36. Dowell, S. J. & Brown, A. J. Yeast Assays for G Protein-Coupled Receptors. *Methods in molecular biology (Clifton, N.J.)* (ed. Filizola, M.) **552**, 213–229 (Springer New York, 2009).
37. Gietz, R. D. & Schiestl, R. H. Quick and easy yeast transformation using the LiAc/SS carrier DNA/PEG method. *Nat. Protoc.* **2**, 35–37 (2007).
38. Eckle, T. *et al.* Cardioprotection by Ecto-5′-Nucleotidase (CD73) and A_{2B} Adenosine Receptors. *Circulation* **115**, 1581–1590 (2007).
39. Li, Q. *et al.* ZM241385, DPCPX, MRS1706 Are Inverse Agonists with Different Relative Intrinsic Efficacies on Constitutively Active Mutants of the Human Adenosine A_{2B} Receptor. *J. Pharmacol. Exp. Ther.* **320**, 637–645 (2007).
40. Guo, Y., Cheng, D., Lee, T. Y., Wang, J. & Hsing, I. New Immunoassay Platform Utilizing Yeast Surface Display and Direct Cell Counting. *Anal. Chem.* **82**, 9601–9605 (2010).
41. Rodríguez, D., Bello, X. & Gutiérrez-De-Terán, H. Molecular modelling of G protein-coupled receptors through the web. *Mol. Inform.* **31**, 334–341 (2012).
42. Esguerra, M., Siretskiy, A., Bello, X., Sallander, J. & Gutiérrez-de-Terán, H. GPCR-ModSim: A comprehensive web based solution for modeling G-protein coupled receptors. *Nucleic Acids Res.* **44**, W455–W462 (2016).
43. Webb, B. & Sali, A. Comparative Protein Structure Modeling Using MODELLER. *Curr. Protoc. Bioinforma.* **47**, 5.6.1-5.6.32 (2014).
44. Stoy, H. & Gurevich, V. V. How genetic errors in GPCRs affect their function: Possible therapeutic strategies. *Genes Dis.* **2**, 108–132 (2015).
45. Sodhi, A., Montaner, S. & Gutkind, J. S. Viral hijacking of G-protein-coupled-receptor signalling networks. *Nat. Rev. Mol. Cell Biol.* **5**, 998–1012 (2004).
46. Bar-Shavit, R. *et al.* G Protein-Coupled Receptors in Cancer. *Int. J. Mol. Sci.* **17**, 1320 (2016).
47. O'Hayre, M. *et al.* The emerging mutational landscape of G proteins and G-protein-coupled receptors in cancer. *Nat. Rev. Cancer* **13**, 412–24 (2013).
48. Beukers, M. W. *et al.* Random Mutagenesis of the Human Adenosine A_{2B} Receptor Followed by Growth Selection in Yeast. Identification of Constitutively Active and Gain of Function Mutations. *Mol. Pharmacol.* **65**, 702–710 (2004).
49. Garcia-Perez, J. *et al.* Allosteric Model of Maraviroc Binding to CC Chemokine Receptor 5 (CCR5). *J. Biol. Chem.* **286**, 33409–33421 (2011).
50. Rodríguez, D., Piñeiro, Á. & Gutiérrez-de-Terán, H. Molecular Dynamics Simulations Reveal Insights into Key Structural Elements of Adenosine Receptors. *Biochemistry* **50**, 4194–4208 (2011).
51. Jespers, W. *et al.* Structural mapping of adenosine receptor mutations: ligand binding and signaling mechanisms. *Trends Pharmacol. Sci.* **39**, 75–89 (2017).
52. Warne, T. *et al.* Structure of a β_1-adrenergic G-protein-coupled receptor. *Nature* **454**, 486–491 (2008).
53. Mariani, R. *et al.* CCR2-64I polymorphism is not associated with altered CCR5 expression or coreceptor function. *J. Virol.* **73**, 2450–9 (1999).
54. Saita, Y. *et al.* Structural Basis for the Interaction of CCR5 with a Small Molecule, Functionally Selective CCR5 Agonist. *J. Immunol.* **177**, 3116–3122 (2006).
55. Deupi, X. *et al.* Structural Models of Class A G Protein-Coupled Receptors as a Tool for Drug Design: Insights on Transmembrane Bundle Plasticity. *Curr. Top. Med. Chem.* **7**, 991–998 (2007).

56. Boulais, P. E., Escher, E. & Leduc, R. Analysis by substituted cysteine scanning mutagenesis of the fourth transmembrane domain of the CXCR4 receptor in its inactive and active state. *Biochem. Pharmacol.* **85**, 541–550 (2013).
57. Fan, Z.-C. & Tao, Y.-X. Functional characterization and pharmacological rescue of melanocortin-4 receptor mutations identified from obese patients. *J. Cell. Mol. Med.* **13**, 3268–3282 (2009).
58. Palczewski, K. *et al.* Crystal Structure of Rhodopsin : A G Protein – Coupled Receptor. *Science.* **289**, 739–745 (2000).
59. Visiers, I., Ballesteros, J. A. & Weinstein, H. Three-dimensional representations of G protein-coupled receptor structures and mechanisms. in *Methods in Enzymology* **343**, 329–371 (2002).
60. Peeters, M. C., van Westen, G. J. P., Li, Q. & IJzerman, A. P. Importance of the extracellular loops in G protein-coupled receptors for ligand recognition and receptor activation. *Trends Pharmacol. Sci.* **32**, 35–42 (2011).
61. Ahuja, S. *et al.* Helix movement is coupled to displacement of the second extracellular loop in rhodopsin activation. *Nat. Struct. Mol. Biol.* **16**, 168–175 (2009).
62. Ongini, E., Dionisotti, S., Gessi, S., Irenius, E. & Fredholm, B. B. Comparison of CGS 15943, ZM 241385 and SCH 58261 as antagonists at human adenosine receptors. *Naunyn. Schmiedebergs. Arch. Pharmacol.* **359**, 7–10 (1999).
63. de Zwart, M. *et al.* Potent antagonists for the human adenosine A_{2B} receptor. Derivatives of the triazolotriazine adenosine receptor antagonist ZM241385 with high affinity. *Drug Dev. Res.* **48**, 95–103 (1999).
64. de Ligt, R. A. F., Rivkees, S. A., Lorenzen, A., Leurs, R. & IJzerman, A. P. A "locked-on," constitutively active mutant of the adenosine A_1 receptor. *Eur. J. Pharmacol.* **510**, 1–8 (2005).
65. Lane, J. R. *et al.* A novel nonribose agonist, LUF5834, engages residues that are distinct from those of adenosine-like ligands to activate the adenosine A_{2B} receptor. *Mol. Pharmacol.* **81**, 475–487 (2012).
66. Sherbiny, F. F., Schiedel, A. C., Maass, A. & Müller, C. E. Homology modelling of the human adenosine A_{2B} receptor based on X-ray structures of bovine rhodopsin, the beta2-adrenergic receptor and the human adenosine A_{2A} receptor. *J Comput Aided Mol Des* **23**, 807–828 (2009).
67. Xu, F. *et al.* Structure of an Agonist-Bound Human A_{2A} Adenosine Receptor. *Science.* **332**, 322–327 (2011).
68. Lebon, G., Edwards, P. C., Leslie, A. G. W. & Tate, C. G. Molecular Determinants of CGS21680 Binding to the Human Adenosine A_{2A} Receptor. *Mol. Pharmacol.* **87**, 907–915 (2015).
69. Liu, W. *et al.* Structural basis for allosteric regulation of GPCRs by sodium ions. *Science.* **337**, 232–236 (2012).

Supplementary Information

Table S1. Expression levels of wild-type and mutant human adenosine A_{2B} receptors. Values are shown as mean ± SD from at least three individual experiments.

	Expression level (%)	
Mutation	**Western Blot**	**Yeast ELISA**
Wild-type	100	100
vector	-	-
C167Y^{ECL2}	76 ± 7	36 ± 11
D148G^{ECL2}	86 ± 1	90 ± 36
F259S$^{6.60}$	83 ± 37	66 ± 30
Y113F$^{34.53}$	143 ± 40	101 ± 52
R215H$^{5.71}$	92 ± 49	86 ± 51
C29R$^{1.54}$	123 ± 34	102 ± 22
F59L$^{2.56}$	111 ± 8	76 ± 26
W130C$^{4.50}$	200 ± 53	40 ± 6
F141L$^{4.61}$	58 ± 9	119 ± 20
Y202C$^{5.58}$	126 ± 20	144 ± 38
P249L$^{6.50}$	91 ± 43	179 ± 38
L310P$^{8.63}$	103 ± 14	92 ± 20
L310F$^{8.63}$	109 ± 24	101 ± 39
L310I$^{8.63}$	121 ± 42	124 ± 30
V315G$^{8.68}$	100 ± 16	205 ± 81

Table S2. Additional characterization of wild-type adenosine A_{2B} receptor and mutant receptor V315G$^{8.68}$ in yeast liquid growth assay and ELISA. pEC_{50} and E_{max} values are shown as mean ± SD from three individual experiments, each performed in duplicate. Yeast ELISA values are shown as mean ± SD from four individual experiments.

Mutations	**pEC_{50}**	**E_{max}**	**Yeast ELISA**
Wild-type	6.84 ± 0.05	100 ± 3	100
V315G$^{8.68}$	7.01 ± 0.05	101 ± 2	102 ± 23

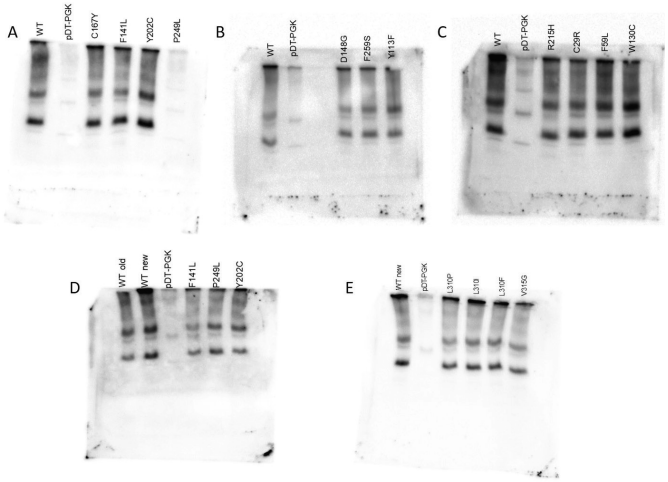

Supplemental Fig. Representative Western blots used in **Fig. 2** for (A) wild-type (WT), vector (pDT-PGK), C167Y, F141L and Y202C, (B) D148G, F259S and Y113F, (C) R215H, C29R, F59L and W130C, (D) P249L and (E) L310P, L310I, L310F and V315G.